UNIVERSIDAD COMPLUTENSE DE MADRID

FACULTAD DE CIENCIAS FÍSICAS

Máster en Astrofísica

TRABAJO DE FIN DE MÁSTER

Evolución dinámica de estrellas con planetas en nuestra Galaxia

Dynamical evolution in the Galaxy of planet-hosting stars

Juan José García Delgado

Supervisado por:

Dra. Isabel Rebollido Vázquez
(European Space Agency)

Dra. Maria Luiza Linhares Dantas
(Pontificia Universidad Católica de Chile)

Curso académico 2024-25

Calificación: 9.0

Contents

Abstract

Context. As stars orbit the Galaxy, their trajectories are perturbed by gravitational interactions with the Milky Way's major structures, such as the bar, spiral arms, and giant molecular clouds. While the dynamical influence of these structures on stellar motion is relatively well understood, their effects on planetary systems remain unexplored.

Aims. Our aim is to investigate the influence of stellar migration on stars' planets. Specifically, we seek to determine whether stars hosting detected exoplanets have migrated from their birthplaces and how such migration may have affected planet formation or survival processes.

Methods. We built a complete catalogue via a crossmatch between the exoplanet.eu and *Gaia* DR3, and complemented with infrared photometries from 2MASS and AllWise. Distances were estimated using a Bayesian method, 3D extinctions were calculated using different dust maps of the Galaxy, and ages were computed using isochrones fitting using PARSEC tracks. Orbital dynamics were integrated using GALPY.

Results. We constructed a consistent catalogue enabling detailed study of planetary systems. Essential parameters for analysing stellar motion were gathered, along with derived estimates such as distances, 3D extinction and stellar ages. Orbital dynamics were reconstructed for a final sample of 1780 stars with a complete set of parameters. Our final catalogue consists of a combination of stellar ($T_{\rm eff}$, $\log g$, [M/H], and so on) and dynamic properties derived from the orbital integration (guiding, apocentric, pericentric radii; eccentricities; angular momentum and action components, to mention a few) for our planet-hosting stars. Additionally, we also have parameters for their planets (such as masses, radii and orbital periods).

Conclusions. With our final catalogue, we move toward assessing the impact of stellar migration on planetary occurrence. The next phase entails estimating birth radii for our sample and comparing those with our derived guiding radii (as well as other dynamic parameters). This phase of the investigation is ongoing. As key deliverables, this project will result in a forthcoming publication and the public release of our compiled catalogue to the scientific community through the CDS.

Key words. Planetary systems – Stars: fundamental parameters – Galaxy: kinematics and dynamics – Galaxy: stellar content – Galaxy: evolution – Methods: statistical

Resumen

Contexto. A medida que las estrellas orbitan la Galaxia, sus trayectorias se ven perturbadas por interacciones gravitatorias con las principales estructuras de la Vía Láctea, como la barra, los brazos espirales y las nubes moleculares gigantes. Aunque la influencia dinámica de estas estructuras en el movimiento estelar se conoce relativamente bien, sus efectos sobre los sistemas planetarios permanecen inexplorados.

Objetivos. Nuestro propósito es investigar la influencia de la migración estelar en los planetas de las estrellas. En concreto, tratamos de determinar si las estrellas que albergan exoplanetas detectados han migrado desde sus lugares de origen y cómo dicha migración puede haber afectado a los procesos de formación o supervivencia planetaria.

Métodos. Construimos un catálogo completo mediante un *crossmatch* entre el exoplanet.eu y *Gaia* DR3, y lo complementamos con fotometría en el infrarrojo de 2MASS y AllWise. Las distancias fueron estimadas mediante un método bayesiano, las extinciones 3D se calcularon utilizando diferentes mapas de polvo de la Galaxia, y las edades se determinaron mediante ajuste de isocronas usando trayectorias de PARSEC. La dinámica orbital se integró utilizando GALPY.

Resultados. Construimos un catálogo consistente que permite el estudio detallado de sistemas planetarios. Se recopilaron parámetros esenciales para analizar el movimiento estelar, junto con estimaciones derivadas como distancias, extinción 3D y edades estelares. Se reconstruyó la dinámica orbital para una muestra final de 1780 estrellas con un conjunto completo de parámetros. Nuestro catálogo final consiste en una combinación de propiedades estelares ($T_{\rm eff}$, $\log g$, [M/H], etc) y dinámicas derivadas de la integración orbital (radios guía, apocéntrico, pericéntrico; excentricidades; componentes de momento angular y de acción, por mencionar algunas) para nuestras estrellas albergando planetas. Además, también disponemos de parámetros de los planetas (como masas, radios y periodos orbitales).

Conclusiones. Con nuestro catálogo final, pasamos a evaluar el impacto de la migración estelar en la formación de planetas. La siguiente fase consiste en estimar los radios de nacimiento de nuestra muestra y compararlos con los radios guía derivados (así como con otros parámetros dinámicos). Esta fase de la investigación está en curso. Como aportaciones clave, este proyecto dará lugar a una publicación próxima y a la difusión pública de nuestro catálogo compilado, disponible para la comunidad científica a través del CDS.

Palabras clave. Sistemas planetarios – Estrellas: parámetros fundamentales – Galaxia: cinemática y dinámica – Galaxia: contenido estelar – Galaxia: evolución – Métodos: estadísticos

1 Introduction

The Milky Way's (MW) large-scale structures continuously alter stellar motions through dynamical processes that may fundamentally shape planetary systems. Three key mechanisms dominate this evolution: *churning* (which alters stellar angular momentum; also known as *radial migration*) and *blurring* (kinematic heating preserving angular momentum; see, for instance, Sellwood & Binney, 2002; Lépine et al., 2003; Roškar et al., 2008, 2012; Kordopatis et al., 2015; Feltzing et al., 2020; Carr et al., 2022; Nepal et al., 2024, and references therein), but also lack of motion disturbance (most likely in the case of younger objects, which have not yet had enough time to interact with the MW's main structures; e.g. Dantas et al., 2025). While these processes are well-characterised in Galactic dynamics, their planetary consequences remain poorly understood, particularly whether they influence planet formation efficiency, system architectures or even promote planetary disconnection through increased free-floating planet rates.

The growing census of exoplanets now enables unprecedented exploration of how Galactic environment affects planetary evolution. Beyond established correlations with local stellar properties like metallicity (e.g. Fischer & Valenti, 2005), little is known about how radial migration through the Galaxy affects the architectures of planetary systems. Such radial motion, which might lead to stellar encounters and interactions with harsh interstellar medium (ISM) environments (e.g. radiation fields from massive stars), could significantly affect the evolution of protoplanetary discs or even impact the gravitational connection between them and their hosting stars — potentially increasing the cases of free-floating planets.

Notably, our own Sun's metallicity is higher than the local ISM (e.g. Wielen et al., 1996; Frankel et al., 2018). This suggests that the Sun also moved to its current location from the inner Galaxy (Baba et al., 2023, 2024; Lu, Yuxi et al., 2024), from approximately 7 kpc to its current 8.2 kpc Galactocentric distance (e.g. Minchev et al. 2013, 2018; Dantas et al. 2025, but see also McMillan 2017 for the current Sun's Galactocentric distance). The Sun's migration has left imprints in Earth's geological record, demonstrating how stellar motion can influence planetary climate (Tsujimoto & Baba, 2020). This serves as motivation to understand what might happen to exoplanets as their host stars' motion is impacted by the MW's major structures.

It is believed that the Sun was born in a clustered stellar environment, where close encounters with other stars likely played a role in shaping the outer Solar System — potentially carving the Kuiper belt, capturing objects like Sedna or explaining the abundance of irregular moons. This would have occurred shortly after the formation of the giant planets ($\sim$ 20 Myr), which present higher occurrence rates in the inner Galactic disc (Baba et al., 2023) — which forms earlier and undergoes faster metal enrichment according to the inside-out galaxy formation scenario (see, for instance, Chiappini et al., 2001; Kobayashi et al., 2006; Magrini et al., 2009; Schönrich & McMillan, 2017; Magrini et al., 2023, to mention a few) — but right before the Sun left its birth cluster (e.g. Portegies Zwart & Huang, 2025, and references therein).

Similarly, the Sun's siblings have dispersed throughout the Galaxy, with an estimated few dozen still located within 100 pc of the Sun (Portegies Zwart, 2009), and it is plausible that some of them could host exoplanets under similar conditions, potentially even favourable to the presence of life. However, it is not this kinship that dictates Galactic habitability, but rather the migratory path of these stars, which plays a more decisive role than either birthplace or current location. Even two stars born at similar Galactocentric radii and currently located at the same distance from the Galactic centre may have experienced vastly different environments during their journeys, significantly impacting the formation and evolution of their planetary systems (Baba et al., 2024).

While the dynamical history of our Sun has been studied in more detail, no systematic study has yet connected stellar motion/migration to their exoplanet populations across the Galaxy. We attempt at bridging this gap through a chemo-dynamic analysis of planet-hosting stars. To that end we recover the data in the exoplanet.eu catalogue, with the goal of comparing current guiding radii (by combining precise astrometry from *Gaia* DR3 and orbit integration from GALPY; Bovy 2015) with birth radii estimates considering chemical enrichment models (similarly to the work developed by Dantas et al., 2025). This methodology allows us to quantify how far stars (and their planets) have migrated from their formation sites — a crucial metric for testing how Galactic dynamics affects planetary systems.

This work unifies three pillars of modern astrophysics: (I) *Galaxy evolution*, connecting orbital dynamics through the influence of major Galactic structures (bar, spiral arms, giant molecular clouds) to exoplanet demographics and survival; (II) *Galactic archaeology*, using stellar chemo-dynamics to trace motion and stellar properties which can be associated with their orbiting planets; and (III) *exoplanet science*, contextualising planets within their Galactic journey. Our study addresses three key questions:

1. How does planetary occurrence vary with stellar motion (i.e. having been churned, blurred or staying undisturbed)?
2. Do dynamically undisturbed/blurred systems show distinct planet populations compared to those that underwent churning?
3. Are certain planet types (e.g. hot Jupiters) preferentially found in stars with specific motion histories?

By mapping how dislocation affects planetary systems, we may uncover clues to both the determination of a *Galactic habitable zone* and regions where dynamics could potentially promote planet detachment (see, for instance, Dayal et al., 2015; Stojković et al., 2019, as references for Galactic habitable zone discussion). Our approach, combining cutting-edge chemical enrichment models with dynamical tools (like GALPY, Bovy 2015), offers the first comprehensive view of how the MW's evolution has sculpted planetary systems from their birthplaces to present-day architectures. Moreover, as a consequent output, we deliver a self-consistent and detailed exoplanet catalogue, including stellar and dynamical parameters, relevant for our scientific purposes.

2 Data and methodology

In order to investigate the motion of exoplanet host stars through the Galaxy, we constructed a sample from the exoplanet.eu (Schneider et al., 2011), a comprehensive compilation of confirmed exoplanets and their host stars, sourced from peer-reviewed publications, which is continuously updated. Our sample was retrieved on 07/11/2024, including a total of 7380 (supposedly) confirmed exoplanets. However, this catalogue also registers objects with estimated masses ranging from 13 to 60 Jupiter masses (M_J), most likely brown dwarf companions. For this reason, we will refer to 'exoplanets' as an umbrella term, including all the objects listed in the catalogue. This simplification will allow us to maintain a clearer narrative throughout this work, without affecting the dynamical analysis significantly.

In this catalogue, we have a particularly heterogeneous sample of all the confirmed exoplanets to date, with parameters estimated through different methods, models and observations. Moreover, there is major incompleteness in the available data for many registered planets, including missing stellar identifiers, fundamental parameters or reliable uncertainty estimates. To accurately probe

the dynamic features of our stellar systems (i.e. planets and host stars), we crossmatched our base catalogue from exoplanet.eu with *Gaia* data release 3 (*Gaia* DR3; Gaia Collaboration et al., 2023), to retrieve the necessary parameters for orbit integration (parallaxes, radial velocities, relevant flags and so on). This way, we were able to work with data that is accurate enough, while ensuring that we have a sufficiently consistent sample for our analysis, including orbital integration.

It is worth mentioning that the original goal of this project was to identify stars hosting exoplanets within the stellar sample studied in Dantas et al. (2023, 2025). However, the lack of matches provided an opportunity to explore the complete exoplanet.eu catalogue in greater depth, applying the methodology described in Dantas et al. (2025) to the stars of stars included in the exoplanet.eu catalogue.

2.1 Catalogues cross-match

2.1.1 Coordinates approach

In order to fulfil our goal of understanding migrations of stars with exoplanets, we first attempted a search for planet-hosting stars in the sample studied in Dantas et al. (2023, 2025), where the authors provide a complete catalogue in terms of chemical abundances and dynamic parameters for a stellar sample observed with the *Gaia*-ESO survey (Gilmore et al., 2012; Randich et al., 2013; Gilmore et al., 2022; Randich et al., 2022). To do so, we performed a crossmatch with the exoplanet.eu catalogue. This cross-match was conducted using the ASTROQUERY package (Ginsburg et al., 2019), with a search around the stars' coordinates (RA, DEC). Our goal was to determine whether some of the stars studied in Dantas et al. (2023), with already available migration histories, had observed exoplanets.

Although the registered exoplanets in the basis catalogue (exoplanet.eu) are scattered across the entire sky, the stars considered in the sample from Dantas et al. (2023, 2025) are confined to declinations between $[-80, 0]$ degrees, as shown in Figure 1. An initial search revealed no matches between both samples, with the closest match being over 200 arcsecs, much larger than the ~ 2 arcsec expected and compatible with an exoplanet-hosting star. This is most likely due to the selection function of *Gaia*-ESO (Stonkutė et al., 2016), which favours low-mass main-sequence turn-off (MSTO) stars, contrasting with the brightness of planet hosts detected to date. In other words, the stars observed by *Gaia*-ESO are not bright enough for the current planet detection techniques. Therefore, we decided to reproduce the work in Dantas et al. (2023) with the whole exoplanet catalogue, reproducing orbital dynamics calculations using the information available in the *Gaia* archive.

We moved on to match the entire exoplanet catalogue with the *Gaia* DR3 to obtain the relevant parameters of the host stars needed to reproduce the work in Dantas et al., 2023. This cross-match was performed using a new query, similar to our previous one, around the exoplanets' coordinates, using thresholds of 2, 5 and 10 arcsec radii around the sources. We finally favoured the 2 arcsec limit to avoid spurious matches. We successfully matched 5325 stellar systems out of 7380 exoplanets from the exoplanet.eu catalogue. However, some difficulties were encountered in matching the remaining systems. Even among the matched ones, certain cases present complexities that may suggest binarity or other ambiguous configurations. We illustrate some of these situations in Figure 2.

First, there is a significant number of exoplanet host stars for which the coordinates provided by the exoplanet.eu catalogue do not appear to match any *Gaia* counterpart, not even within a radius slightly larger than 10 arcsec, like exoplanets 8 and 47 in Figure 2. On the other hand,

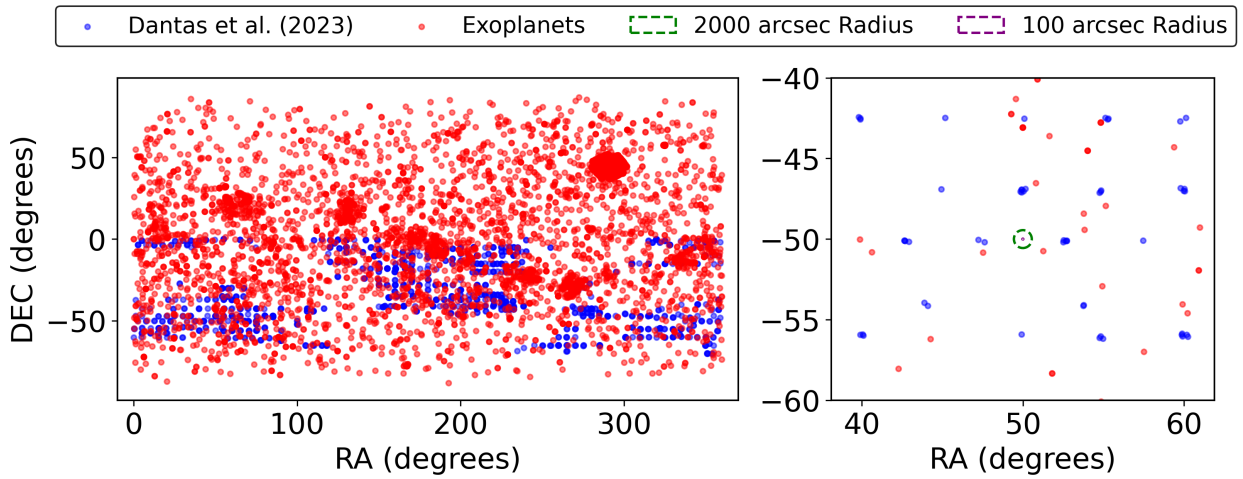

Figure 1: Sky coverage of the exoplanet.eu catalogue (Schneider et al., 2011) and the stars studied in Dantas et al. (2023) is shown on the left, with a zoomed-in view of the region with $-60° < \mathrm{DEC} < -40°$ and $38° < \mathrm{RA} < 62°$ shown on the right, to illustrate the lack of matching targets.

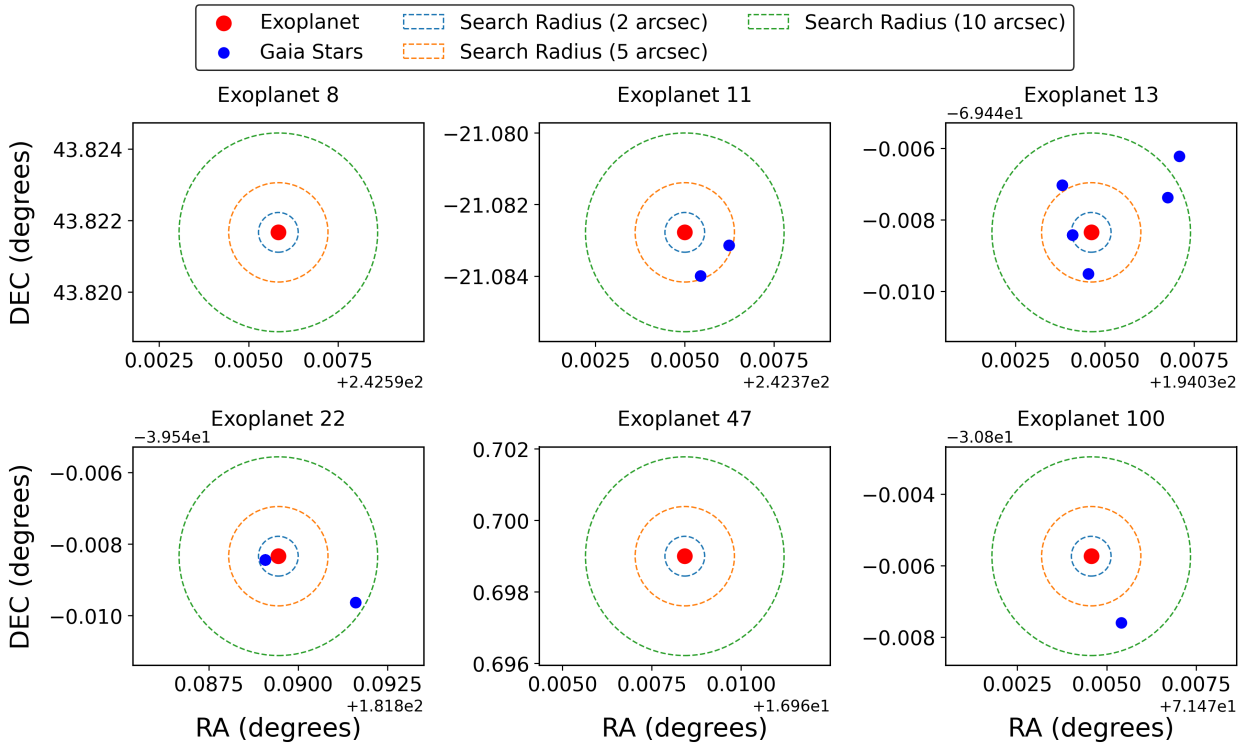

Figure 2: Selected examples of crossmatch attempts between the stars in the exoplanet catalogue and *Gaia* DR3. *Gaia* DR3 stars are shown in blue and planet hosting stars from the exoplanet.eu catalogue are shown in red. The dashed lines mark 2, 5 and 10 arcsec distance from the exoplanet.eu catalogue stars.

there are quite a few cases where stars are located too far away, making the match ambiguous, such as in the cases of exoplanets 11 and 100. Similarly, cases like exoplanet 13 apparently show a candidate star within less than 2 arcseconds, but there are other stars not so far away, which could suggest multiple stellar systems. However, it is true that there are some clear matches, as seen in the example of exoplanet 22, although this is not the most frequent situation in our

sample. Additionally, binary systems could present challenges with this previous approach. Also, it is worth mentioning that we are not including proper motion corrections here, considering the small difference between observation epochs. Although in specific cases this consideration could clarify some ambiguities, this procedure would still not be optimal either. At this point, it seemed worthwhile to avoid potential mismatches by relying on the host star identifiers already provided in the exoplanet.eu catalogue, rather than performing a new crossmatch that could lead to incorrect associations.

2.1.2 Identifiers approach

Given a coordinate match was returning duplicated or even missing matches, we decided to turn to the stellar identifier provided by the exoplanet.eu catalogue as input for automated queries to the SIMBAD website using a PYTHON routine. This would allow us to retrieve from SIMBAD the corresponding *Gaia* identifiers, later referred to as `source_id` in our final catalogue.

In order to optimise the efficiency of this process, we developed a routine that searches for the host stars names for each exoplanet. The exoplanet catalogue includes several identifiers, so we use those potentially leading to a match. Specifically, `star_name` and `star_alternate_names` contain different nomenclatures for the host star, as well as `name` and `alternate_names`, which refer to planet identifiers. Moreover, several names are sometimes included in the same column. This search was also extended by automatically removing planetary and binary suffixes that could hinder SIMBAD identification — for example, the exoplanets named 112 Psc b and UZ For (AB) b, whose stars were found under the names 112 Psc and UZ For. After the SIMBAD query, we extract the Gaia identifier, which enables accurate object identification through a query in the *Gaia* archive, from where we obtain various stellar parameters.

Thus, out of 7380 exoplanets in our sample, we matched 6292 of them with stars observed with *Gaia*. However, the exoplanet catalogue includes 777 objects listed as free-floating exoplanets — i.e. they do not possess an associated star — but we found that this classification might not be accurate. In other words, these exoplanets might not necessarily be free-floating. Although there was no information in the star name columns in these 777 cases, we were able to find a match for 239 of them using the identifiers extracted from other columns such as those referring to exoplanet names. The remaining exoplanets may include some unmatched objects which do have a host star, but it is not possible to match them based on only the identifiers available in the catalogue.

Furthermore, the reasons for the 1088 unmatched exoplanets are varied. In most of these cases, the search in SIMBAD was unsuccessful because we could not find the object in the database using our name candidates. To solve this, we could complement our approach using another coordinates crossmatch. However, in order to maintain consistency and to not include mismatches, we decided not to use this solution initially.

Also, we discovered several issues related to naming inconsistencies, that may be contributing to these missing crossmatches. In some sources, we found errors in the identifiers. For instance, 2MASSW J0030300-145033 was missing the 'W' in the exoplanet catalogue. Additionally, this example contains coordinates information in its name, usual in some astronomical objects, which can lead to no matches in other cases as well. For example, 1SWASP J1407 b cannot be found with this name (even without the 'b' suffix, related to the exoplanet), because the star is listed in SIMBAD as 1SWASP J140752.03-394415.1. In this situation, the no match was due to a truncation of the coordinates in the identifier name. This issue underscores a broader challenge in astrophysics: the absence of a standardised naming convention for celestial objects. While the impact on our work is somewhat small, such inconsistencies could pose significant problems for automated pipelines,

where uniformity is critical for data processing and cross-catalogue matching.

On the other hand, we encountered some cases where the SIMBAD query successfully identified the star, but no *Gaia* DR3 identifier was present for that object. This is possibly due to the limiting magnitude of the *Gaia* instrument for faint sources around $G \approx 21$ and a bright limit of about $G \approx 3$[1]. For example, we found alf Tau and alf Ari in SIMBAD, but they do not have a *Gaia* identifier because they are too bright, with magnitudes $G \approx -0.04$ and $G \approx 1.53$, respectively[2]. On the other hand, there are also some faint sources which fall outside *Gaia*'s magnitude range, such as 4U 1857+01 and XB 1916-053, with magnitudes close to 21.

Having the *Gaia* identifiers at hand, we used them to perform a query in the *Gaia* archive for 4751 stars (hosting 6292 planets) and retrieve their stellar parameters needed for running the integration of orbits (which we describe in detail in Sect. 2.5). This follows the same procedure as before with coordinates, but now using *Gaia* identifiers to facilitate the matching process. The stellar parameters selected were parallaxes (θ), radial velocities ($V_{\rm rad}$), metallicities ([Fe/H]), surface gravities ($\log g$), effective temperatures ($T_{\rm eff}$), ages ($t_\star$) and distances (D). We also estimated the distances using a Bayesian statistical approach (which we describe in Sect. 2.2).

2.2 Zero-point correction for parallaxes and Bayesian distances

To calculate the orbits around the Galactic centre of the planetary systems (stars + planets) in our dataset, an accurate distance estimation is essential. Achieving this requires a zero-point parallax correction to the data. The following steps outline the procedure for both the zero-point correction and the subsequent distance estimation.

We performed the calculation of the parallax zero-point correction for all the stars with sufficient information in our sample — i.e. coordinates (RA, DEC), parallax, proper motions, G-band mean photometric magnitudes, effective number of sources used in astrometry, pseudocolour, ecliptic latitude and number of astrometric parameters resolved. In addition, there are some specific requirements for these parameters to calculate the zero-point correction: `pseudocolor=NaN` or $1.24 <$ `pseudocolor` < 1.72, and `astrometric_params_solved` > 3. These corrections rectify certain systematic offsets noticed in the estimation provided by the *Gaia* mission (Lindegren et al., 2021). The parallax zero-point correction was calculated according to the recipe described in Lindegren et al. (2021)[3].

With the zero-point corrections at hand, the distances were estimated using the corrected parallaxes and the Bayesian approach from Bailer-Jones (2015)[4]. We obtained several distance estimates representing different statistical percentiles and confidence intervals, such as the mode, full width at half maximum (FWHM) bounds and quantiles corresponding to central estimates and various credibility intervals derived from the posterior distribution (percentiles that correspond to 1, 2 and 3σ intervals, assuming a Gaussian distribution for the posteriors). For practical usage, we adopt the median distance as our distance, due to its robustness against outliers. We provide errors and confidence/credible intervals whenever possible.

These Bayesian distances were compared to the ones provided by the *Gaia* pipeline, as shown in Figure 3. Within 2500 pc our Bayesian distance estimates show reasonable agreement with those

[1] See the *Gaia* DR3 description: https://www.cosmos.esa.int/web/gaia/dr3

[2] These G-band magnitudes were estimated using the Johnson-Cousins V and I magnitudes from SIMBAD and applying the transformation equations into the *Gaia* photometric system described in Jordi et al. (2010)

[3] Using the dedicated PYTHON package available here: https://gitlab.com/icc-ub/public/gaiadr3_zeropoint.

[4] We adapted the R recipe available here: https://github.com/bailer-jones/parallax-tutorial-2018 to retrieve the posteriors and their summary statistics.

provided by *Gaia*. The discrepancies observed at larger distances are primarily due to a few outliers. These may be attributed to systematic errors in the *Gaia* pipeline, particularly in the estimations for faint or complex sources. In the case of these outliers, we also compared the distances with those reported in the exoplanet.eu catalogue, when available, and found a significantly better agreement with the Bayesian estimates than with the *Gaia* ones. This supports the reliability of our procedure, particularly in the regime where *Gaia*'s estimations might be affected by certain biases.

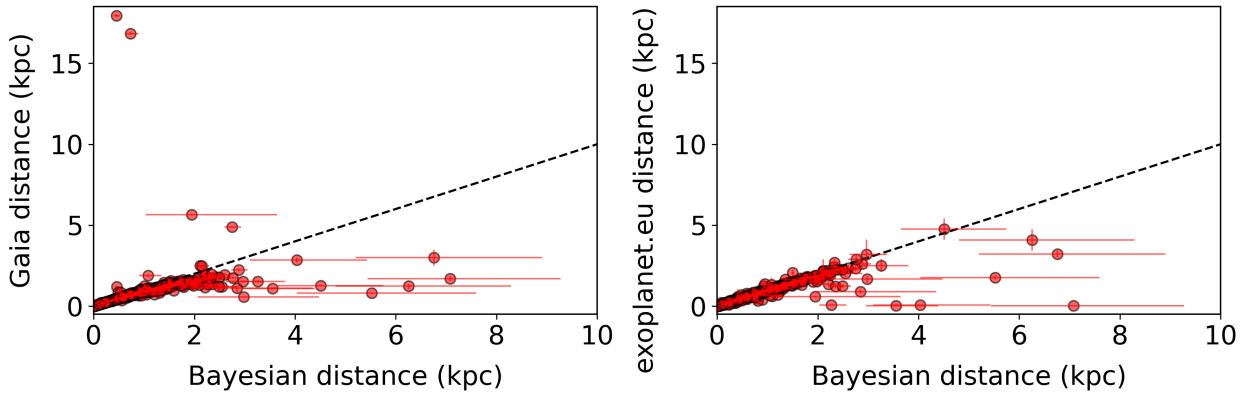

Figure 3: Left panel: Comparison between *Gaia* and our Bayesian distance estimates for 3857 stars hosting 5137 exoplanets. Right panel: Comparison between the exoplanet.eu catalogue and our Bayesian distance estimates for 2428 stars hosting 3556 exoplanets. The dashed line indicates the one-to-one relation to highlight deviations. Error bars represent *Gaia* or exoplanet.eu uncertainties in each case and Bayesian 1σ credible intervals. Note: Although the panels show different stellar subsamples due to distance estimates availability in each case, outliers are present in both of them, ensuring correct performance of the Bayesian procedure.

2.3 3D extinction

2.3.1 3D extinction overview

Interstellar extinction — the absorption and scattering of starlight by dust — is a dominant systematic effect in studies of MW stars. Unlike extragalactic astronomy, where extinction is often treated as a line-of-sight integrated effect (2D), studies of stars in the Galaxy require 3D extinction mapping to account for the spatial distribution of dust between the observer and the target (i.e. dust column). This distinction proves critical for the MW, where stellar distances span orders of magnitude and neglecting the 3D dust distribution systematically biases derived stellar properties, particularly magnitudes and ages. Recent advances in astrometry (e.g. *Gaia*; Gaia Collaboration et al., 2023), photometric surveys and 3D dust modelling (e.g. BAYESTAR; Green et al., 2015, 2018) now enable precise, distance-resolved extinction corrections. These methods are transformative for studies of Galactic structure, stellar populations and the interstellar medium.

In this work, we implement 3D extinction corrections primarily for age-dating stars using UNIDAM (Mints & Hekker, 2017, 2018, which we ultimately discard, due to the reasons discussed in Sect. 2.4), with the same framework being equally applicable to spectral energy distribution (SED) analysis when required. Here we detail our methodology for estimating 3D extinction, including the key steps, current limitations and specific challenges encountered when applying these techniques to our stellar sample.

2.3.2 Extinction estimates for our sample

Since the stars in the exoplanet catalogue are relatively nearby (median distance in the sample ~ 350 pc) due to the limitations of the current most effective planet detection techniques, the effect of 3D extinction should be relatively low. Nevertheless, we estimated the 3D extinction using the DUSTMAPS package (Green, 2018) in the PYTHON environment, more specifically BAYESTAR (Green et al., 2015, 2018) and Edenhofer modules (Edenhofer et al., 2024). Such extinction maps have, however, distinct limitations and, consequently, we made use of both of them to maximise our final sample of stars. The BAYESTAR module provides maps that cover the Pan-STARRS 1 footprint (DEC $> -30°$; i.e. excluding most of the southern sky)[5] amounting to three-quarters of the sky. In the case of the Edenhofer maps, the coverage is limited in distance, reaching out up to 1.25 kpc from the Sun.

Bayestar provides extinction estimates for 3914 stars in our complete sample, while the Edenhofer map covers 3093 stars. In Edenhofer's 3D dust map assembly, the authors used the stellar distance and extinction estimates from Zhang et al. (2023) — which are primarily based on the *Gaia* BP/RP spectra — where extinction uncertainties are lower than competing catalogues while probing a similar number of stars. Also, this map is in good agreement with existing 3D dust maps and improves upon them in terms of volume covered at a high spatial resolution (see Edenhofer et al., 2024). For these reasons, as some stars in our sample are covered by both BAYESTAR and Edenhofer, in case of duplicates, we prioritised those from the Edenhofer map.

Fig. 4 compares the interstellar reddening estimated by the BAYESTAR and Edenhofer 3D dust maps at a distance of 1 kpc. While both maps provide total E(B-V) extinction along each line-of-sight, they differ in methodology and statistical treatment: the BAYESTAR map shows median cumulative reddening, whereas the Edenhofer map presents mean integrated values. Differences in structure and intensity reflect these modelling choices. Fig. 5 shows our 3D extinction estimates obtained using the BAYESTAR and Edenhofer dust maps (top row), respectively, along with the distribution of E(B-V) for each case (bottom row).

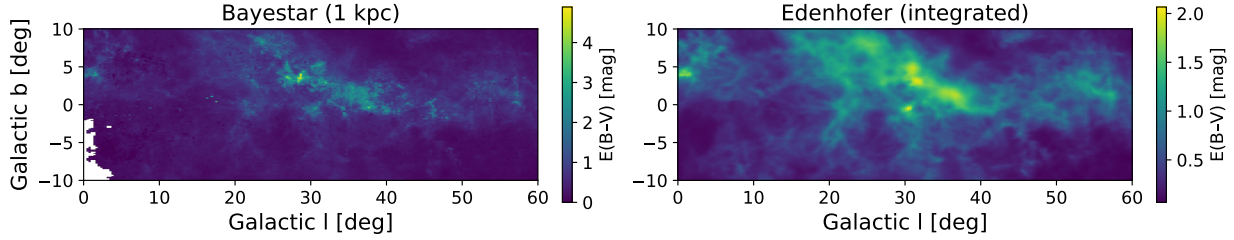

Figure 4: Comparison of interstellar extinction from two 3D dust maps. Left panel: BAYESTAR (Green et al., 2018), showing the *median* cumulative reddening E(B-V) to a distance of 1 kpc, based on stellar photometry and parallax measurements. Right panel: Edenhofer's dust map (Edenhofer et al., 2024), showing the *mean* integrated E(B-V) along the line of sight to 1 kpc, derived from a probabilistic dust model using *Gaia* data. While both maps represent total extinction to the same distance, they differ in methodology and statistical interpretation. Both panels cover Galactic longitude l from 0° to 60° and latitude b from −10° to 10°. These two dust maps were generated using the DUSTMAPS package. Colour scales indicate total reddening in magnitudes. Note that the E(B–V) colour scales differ between the panels to enhance visual contrast.

We now proceed by quantifying the uncertainties for extinction. We derive the 3D extinction using the distributions of the posteriors from the Bayesian distances, considering the median value

[5]See their documentation: https://dustmaps.readthedocs.io/en/latest/modules.html.

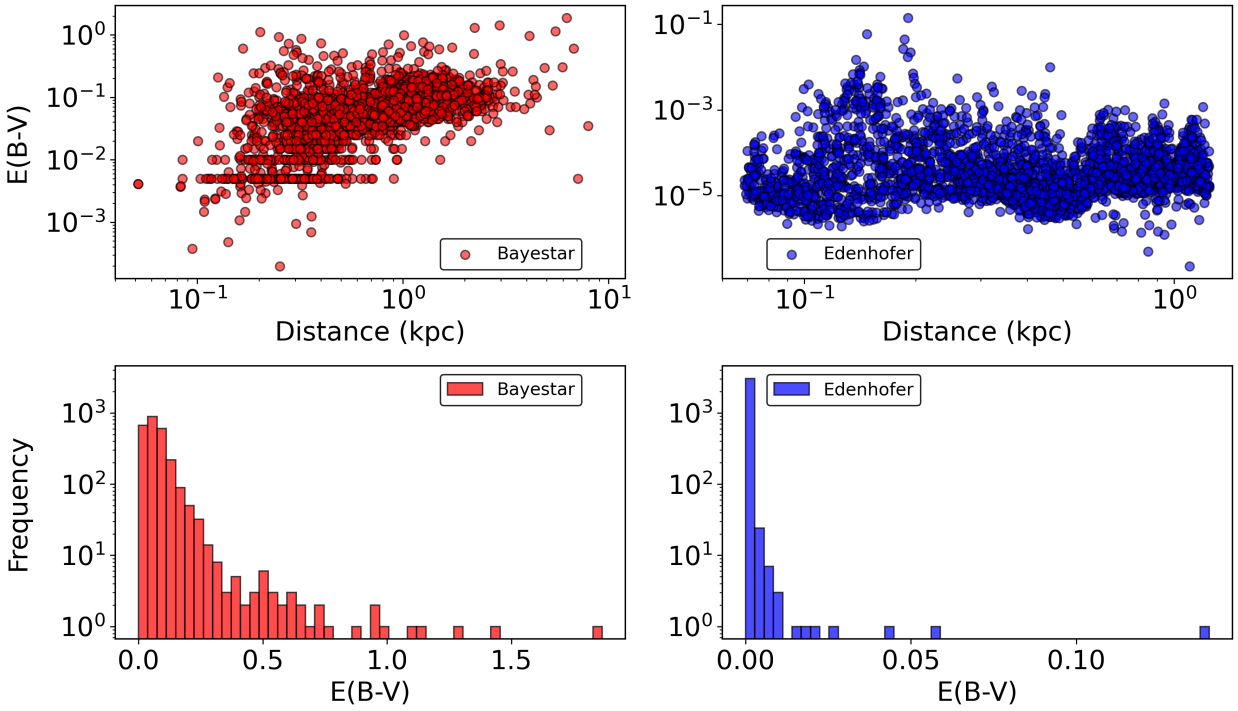

Figure 5: Top panels: Extinction estimates from the BAYESTAR (left; Green et al., 2018) and Edenhofer (right; Edenhofer et al., 2024) 3D dust maps as a function of distance for stars in our complete sample. Bottom panels: Distributions of extinction values from each map. All subplots are depicted in logarithmic scale for enhanced visualisation. BAYESTAR successfully estimated extinction for 3914 stars hosting 5263 exoplanets, while Edenhofer estimated E(B-V) for 3093 stars hosting 4070 exoplanets.

and propagating the distances 1σ credible interval. Nonetheless, we also take into account that the computation of these extinction maps involves associated statistical uncertainties. For this reason, we compared these two different uncertainties and selected the largest, as a conservative choice. However, the statistical uncertainty estimates supplied for BAYESTAR and Edenhofer's extinction maps are computed distinctly. Edenhofer's maps already provide a standard deviation estimate, while when using BAYESTAR we had to estimate an analogous approach using percentile mode, with an 84% value, and considering the difference with the median value obtained. In general, our statistical errors with DUSTMAPS are larger by orders of magnitude than the ones from the confidence intervals propagated from Bayesian distances. Therefore, we again adopt these as a conservative estimate in both cases. Extinction estimates were obtained for a total of 4202 stars hosting 5585 planetary systems.

2.4 Ages estimations

We attempted estimating stellar ages, for which other quantities were essential for running UNIDAM (Mints & Hekker, 2017, 2018), such as 2MASS (JHK bands; Skrutskie et al., 2006) and AllWise ($W1W2$ bands; Cutri et al., 2021) magnitudes, which we retrieved using TOPCAT (Taylor, 2005). To that end, we used a 2 arcsec threshold through the X-match tool. Previously, we calculated the 3D extinction, obtaining estimates for 4202 stars (hosting 5585 exoplanets). Throughout the entire methodology, some stars had to be gradually discarded from the base sample due to the absence of measurements or estimates for certain parameters. Consequently, the number

of stars for which we can perform the orbit calculations differs from this total, as different parameters are required. Ultimately, our final sample would correspond to the intersection of both subsets, including only those stars with both age estimates and computed orbital dynamics. Nevertheless, we estimated ages for as many stars as possible, aiming to generate the broadest and most self-consistent catalogue as possible.

With this procedure, we computed age estimations for 1071 stars. At this point, we lose a significant number of stars from our sample. This is due to missing information in the photometry and/or the fitting procedure embedded within UNIDAM; this limitation is noted by the authors (Mints & Hekker, 2017, 2018). Moreover, in some cases, UNIDAM provides more than one possible solution for a given star, with an additional probability flag. According to Dantas et al. (2023), these solutions can provide degenerate and the values remain quite uncertain. Following their criteria, we retained only stars with a quality flag equal to 1, corresponding to those with a single solution. This results in a total of only 550 stars. Given the low number of stars in this sample, we decided to take one step back to maximize quality and quantity in our final sample. Therefore, we hereafter consider the original age estimations already included in the exoplanet.eu catalogue for our analysis, despite these age values not being calculated in a homogeneous way.

With the information added to our catalogue so far, we can briefly analyse some properties of the sample of stars in this catalogue. Considering surface gravity, temperature and metallicity values from *Gaia*, we can construct a Kiel diagram, shown in Fig. 6. Here we can observe our sample distribution, showing a clear main sequence along with subgroups of more evolved stars. We also overlay representative isochrones considering the range of metallicities involved in our final sample of stars.

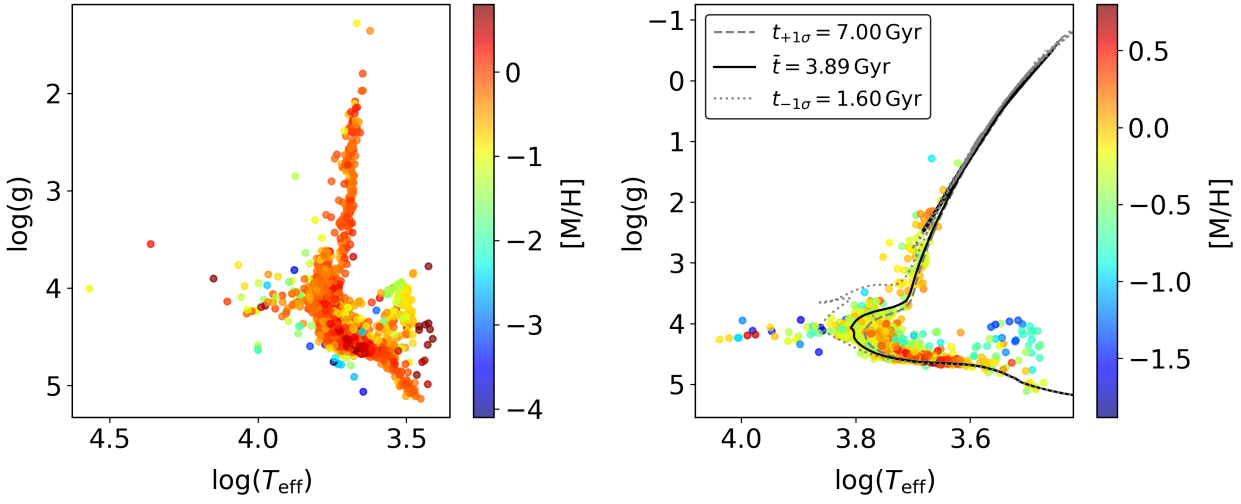

Figure 6: Left panel: Kiel diagram showing all stars from the exoplanet.eu catalogue successfully crossmatched with *Gaia* DR3 and with available $\log g$, $T_{\rm eff}$ and [M/H] estimations, involving 3853 stars hosting 5155 exoplanets. Right panel: Kiel diagram depicting the final sample indicated in Sect. 2.6, using age estimates from the exoplanet.eu catalogue, but also considering *Gaia* DR3 provided estimations for the parameters involved. The isochrones shown were computed using PARSEC stellar tracks (Bressan et al., 2012); the evolutionary tracks shown correspond to the median age (continuous line) and $\pm 1\sigma$ (dashed lines), with metallicity fixed at the median value ($\langle$[M/H]$\rangle = -0.12$) for our final sample.

2.5 Orbits estimations

Stellar orbits were integrated using GALPY (Bovy, 2015) with the Galactic gravitational potential from McMillan (2017) and 10 Gyr lookback time. Since GALPY does not natively provide uncertainty estimates, we implemented a resampled the data to propagate observational errors:

1. **Input Parameters:** The integration requires:
   - Astrometric quantities: RA, DEC, proper motions (along with their respective uncertainties), from *Gaia* DR3.
   - Radial velocities from *Gaia* DR3.
   - Distance estimates: median distance and associated uncertainty ($\pm 1\sigma$), based on zero-point-corrected *Gaia*DR3 parallaxes and derived from our Bayesian approach.
   - Solar position and motion assumptions.
2. **Resampling:** We quantified orbital integration uncertainties through a two-stage resampling procedure. First, we generated 100 realisations for each star by independently sampling each input parameter from its Gaussian error distribution $\mathcal{N}(\mu_i, \sigma_i^2)$. Second, we performed an additional 100 multivariate normal samplings to properly account for parameter covariances. This dual sampling strategy propagates both individual measurement errors and their correlations through the orbit integration, yielding robust error estimates for all derived quantities. Final confidence intervals were computed empirically from the full distribution of resampled outcomes.
3. **Dynamical Parameters:** From the orbit integrations, we derived:
   - Orbital eccentricities (e);
   - Maximum Galactic scale heights ($Z_{\rm max}$);
   - Heliocentric distances (x, y, z);
   - Total binding energy (E_t) and energy components (E_r, E_z);
   - Velocity components in both Cartesian and cylindrical coordinates (v_x, v_y, v_z, v_r, v_ϕ);
   - Local standard of rest velocity components (U, V, W);
   - Angular momentum components (L_x, L_y, L_z);
   - Orbital action components (J_r, J_ϕ, J_z);
   - Pericentric/apocentric distances ($R_{\rm peri}$, $R_{\rm apo}$);
   - Guiding radius ($R_{\rm g}$).

The final values were taken as the median from the bootstrap, with uncertainties ($\pm 1\sigma$) derived from the 16th and 84th percentiles. We will refer to the median values of each parameter (e.g. $\langle e \rangle$ for eccentricity) throughout the analysis. This approach accounts for observational errors but neglects potential systematic uncertainties in the gravitational potential itself.

To integrate these orbits, we made use of the High-Throughput Computing (HTC) services provided by the GUAIX group from the Departamento de Física de la Tierra y Astrofísica at the Universidad Complutense de Madrid. To efficiently perform the orbit integration for the largest subsample of stars — i.e., those with all required parameters available — we parallelised the computation by running an adapted version of the orbit integration code individually for each star on the HTC cluster. The routine was modified to optimise its performance within an HTC environment. A total of 3308 jobs were submitted — one per star in the sample — and distributed across more than 40 different nodes. Each job generated a file containing the dynamical parameters obtained from the resampling, from which we extracted their median values as estimates.

2.6 The final sample

Our final sample is comprised of 1780 stars hosting 2281 exoplanets, selected from the subset of 3308 stars with computed orbits. This reduction in sample size guarantees that both parameter coverage and sample size are respected for an optimal scientific investigation. The exclusion of stars is mostly due to the lack of sufficient stellar parameters, which are necessary for the subsequent analysis, such as metallicities from *Gaia* DR3 and ages from the exoplanet.eu catalogue. The sample size at each stage of our procedure is depicted in Fig. 7 in order to facilitate comprehension of the methodology.

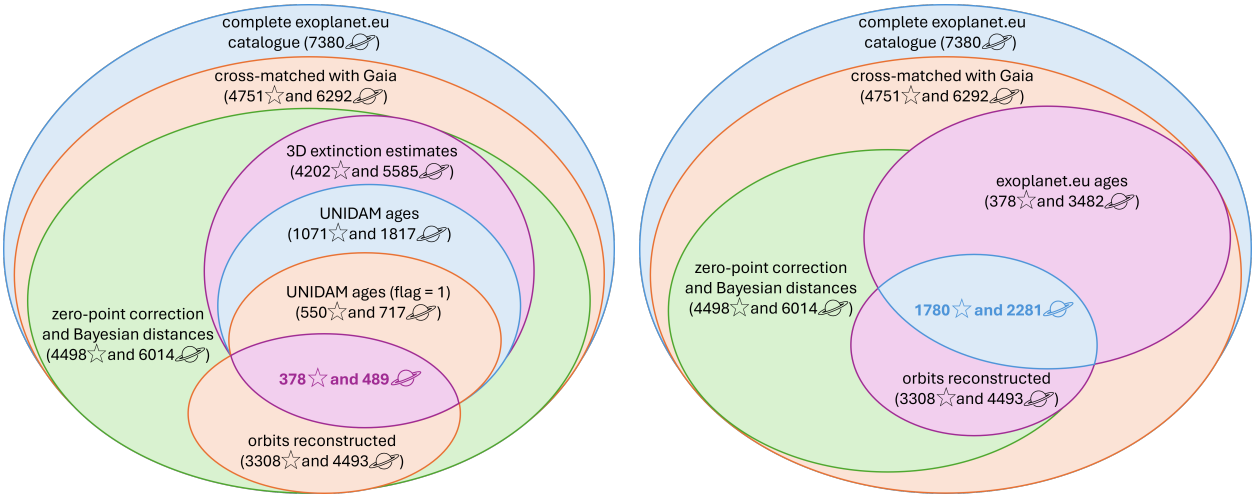

Figure 7: Diagrams showing the samples size progression through the successive steps detailed in Sect. 2. Both panels illustrate the interactive process to acquire a complete sample in terms of parameter coverage and sample size. Left panel: final sample obtained using UNIDAM age estimates, which was ultimately discarded. Right panel: final sample used in the analysis, based directly on the exoplanet.eu catalogue ages. The right panel depicts the actual final sample used for our study hereafter.

Our adoption of age estimates from the exoplanet.eu catalogue, rather than homogeneous determinations via UNIDAM, represents an optimal balance between sample size and parameter consistency. While UNIDAM ages would improve internal uniformity and consistency, their application — when combined with other necessary sample filters — would drastically reduce our stellar sample by 79% (from 1780 to just 378 stars). This severe reduction could disproportionately affect rare dynamical populations and their exoplanets, potentially biasing our statistical conclusions about migration/motion effects within the Galaxy. The catalogue ages maximise both sample size and the full chemo-dynamic parameter space needed for robust population analysis.

3 Preliminary results and discussion

In this Section, we start by examining some parameters and properties of our final sample. The distributions of some of these parameters are shown in Fig. 8. Scatter plots depicting some expected or interesting potential relations are shown in Fig. 9.

We observe that the stellar parameters of our final sample are clearly distributed more or less around the solar values (as depicted by the dashed lines), not to mention that the bulk of our stellar sample is comprised of FGK-type stars (as shown by the distribution of temperatures in

the left lower corner of Fig. 8), with a median of $\sim$ 5600 K (which is very close to the solar effective temperature: $T_{\rm eff,\odot} = 5773 \pm 16$; Asplund et al., 2021) and values ranging from 3000 to 10900 K. On average, the stars in our final sample are slightly younger than the Sun (the Sun's age being $t_\odot = 4.775 \pm 0.039$ Gyr, as shown by Bonanno & Fröhlich, 2015, see their final estimate from their Table 3, which the authors regard as the most potentially accurate), with a median age of 3.89 Gyr, while the youngest star is only about 0.4 Myr and the oldest approaching 15 Gyr. Their typical metallicity being lower than the Sun, with a median value of $\langle$[M/H]$\rangle = -0.12$ (as previously indicated in Fig. 6), with values ranging between -1.88 and 0.80[6]. The Sun itself, by definition, has [M/H]=0, but [Fe/H] could be as high as 0.03 dex (as estimated through non-local thermodynamic equilibrium corrections performed by Korn et al., 2003). Both stellar masses and radii are close to the solar values, with median values of 1.03 $M_\odot$ (full range being [0.02, 2.89]) and 1.09 $R_\odot$ (full range being [0.17, 88.5]). In terms of distance, most stars lie within a few hundred parsecs (median $\approx$ 300 pc), with the closest at $\sim$ 2 pc and the farthest located at $\sim$ 3.5 kpc.

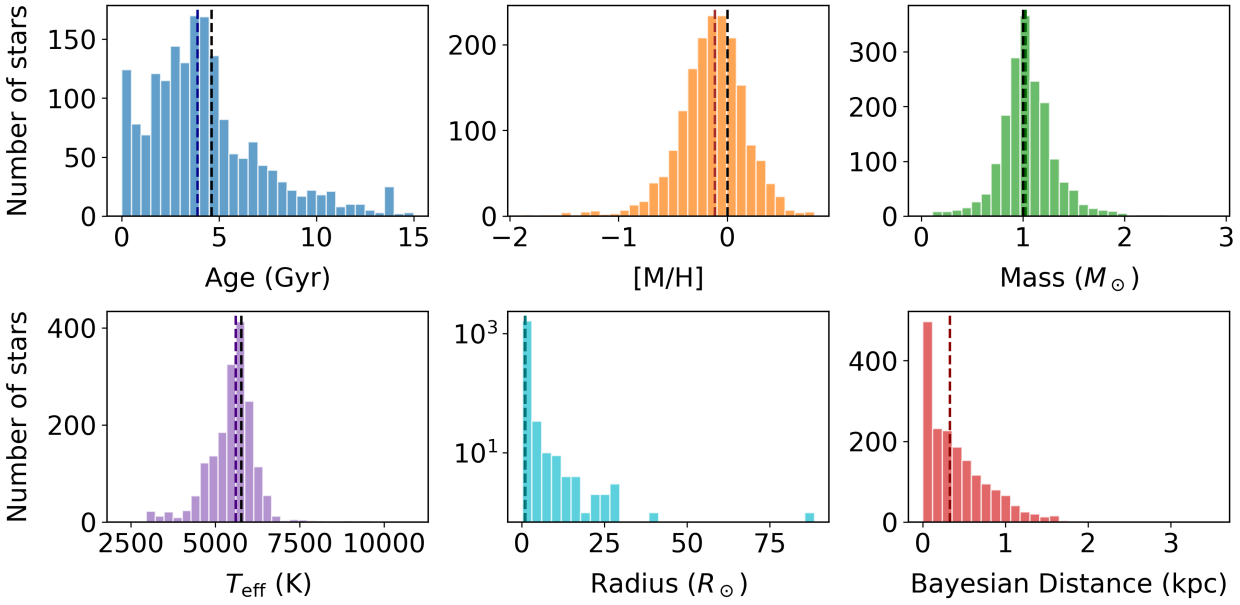

Figure 8: Distributions of five fundamental stellar parameters in our final sample of stars: age, metallicity, mass, effective temperature and radius. Each distribution includes a vertical black dashed line indicating the Sun's reference value for comparison, and a coloured dashed line indicating the median value of the corresponding parameter in the final sample. The distribution of the estimated Bayesian distance to those stars is also included. Note the logarithmic scale in the radius histogram.

These properties likely reflect potential biases. These stars present confirmed exoplanets, which implies, for instance, that they are both close and bright enough to allow detection — though the brightest ones were excluded during the crossmatch with *Gaia* DR3 due to magnitude limitations (see Sect. 2.1.2). Also, there are additional biases depending on the detection techniques used. For example, transit detections are biased toward compact systems, while radial velocity methods perform better on stars with slow rotation and low activity.

Next, we investigate possible relations among these key stellar properties in Fig. 9, in search of some trends or groupings. For instance, in the stellar mass versus age plot, we find a generally negative trend, with massive stars clustered at lower ages and less massive ones spanning a wider

[6]Upon a more careful inspection, we verified that this supposedly extremely metal-rich star with [M/H]=0.8 is a high proper motion star. The metallicity estimate for this object according to the exoplanet.eu is 0.35.

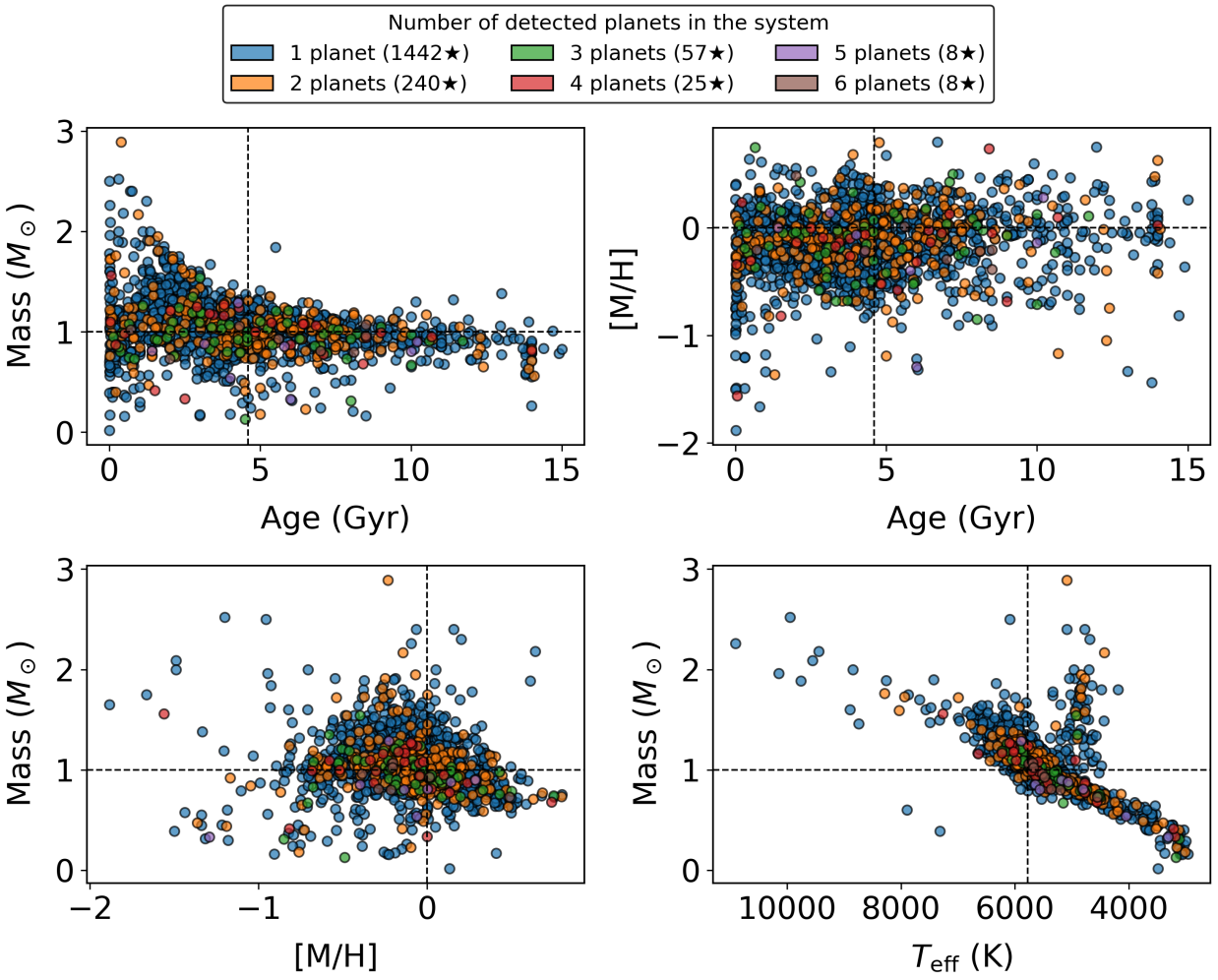

Figure 9: Pairwise plots of four fundamental stellar parameters in our final sample of stars: age, metallicity, mass and effective temperature. Points are coloured by the number of detected planets per system. The legend depicts in parentheses the number of stars hosting a given number of planets. Black dashed lines indicate the Sun's reference values for comparison.

age range. This behaviour is consistent with stellar evolution theory, as more massive stars consume their nuclear fuel faster, which results in shorter lifetimes and higher luminosities (see, for instance, Chieffi et al., 1998; Groh et al., 2014; Haemmerlé et al., 2019). On the other hand, the mass versus temperature plot — analogous to a colour-magnitude or Kiel diagram — shows a direct dependence, where higher mass corresponds to higher temperature. This is again consistent with what one would expect from stellar evolution theory and other observational studies (e.g. Eker et al., 2018; Evans et al., 2023). Additionally, we also display the number of detected exoplanets per stellar system. We observe that the prevalence of planets hosted by massive stars is small; systems with multiple exoplanets tend to happen more frequently in stars with solar-like masses. These trends reflect the effects of the rapid dispersal of protoplanetary discs in high-mass stars, limiting planet formation time (see, for instance, Alexander et al., 2014; Picogna et al., 2021; Komaki et al., 2023), also combined with observational biases favouring the detection of exoplanets in low-mass stars. We will explore these trends in more detail in the next steps of our investigation.

It is worth mentioning that our final sample includes 2281 'exoplanets', of which 1299 have masses below 13 M_J, in agreement with the standard definition of exoplanet. In contrast, 121

exceed this threshold ($M > 13M_J$) and should be considered as brown dwarfs. The remaining 861 exoplanets have no reported masses. Given the limitations of current detection methods — primarily radial velocity and transits — accurate planet masses are often difficult to determine. Radial velocities yield only a minimum mass ($M \sin i$), which depends on the unknown orbit inclination i. Transits, while providing planetary radii, do not directly measure mass, although modelling of Transit Timing Variations (TTVs) can be used to estimate planetary masses in multi-planet systems (see, for instance, Ofir et al., 2025). Nevertheless, *Gaia* DR4 will allow better mass estimations thanks to upcoming new astrometric data [7].

In Fig. 10, we observe that low-mass planets are more abundant across the sample, while more massive planets tend to orbit stars with solar-like metallicity, which aligns with the well-established correlation between giant planet formation and metal-rich environments (Santos et al., 2001; Haywood, 2009).

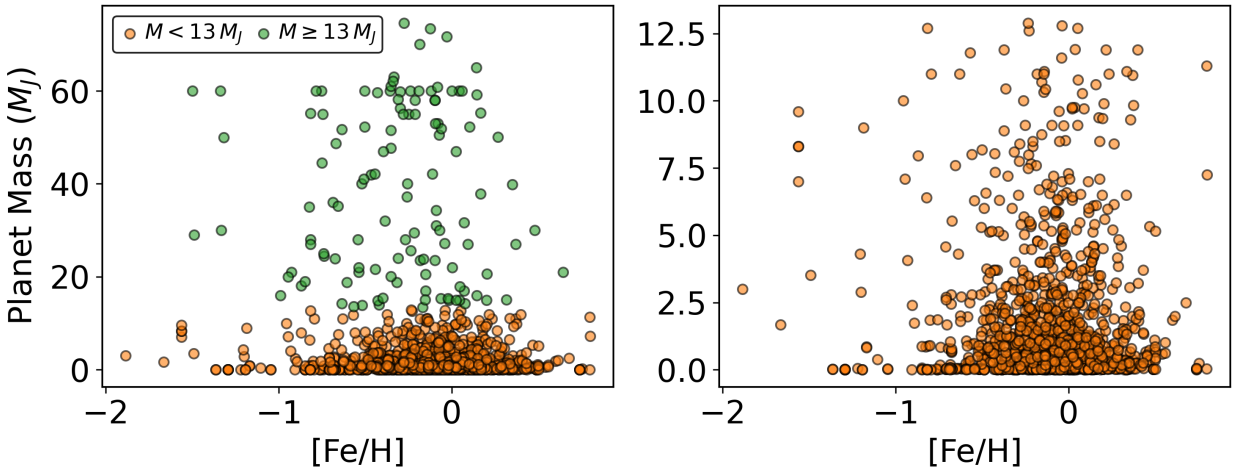

Figure 10: Masses of the 'exoplanets' (those with $M > 13M_j$ are considered brown dwarfs by definition) as a function of the metallicity of their host stars. Left panel: All cases with reported mass values, distinguishing between exoplanets (orange) and brown dwarfs (green), according to their mass ranges. Right panel: Same plot but restricted to only objects meeting the mass criterion for exoplanets. Note that the planet mass range is different for each subplot to allow for a better visualisation.

We now describe some of the preliminary results from the orbit integration applied to our sample. Fig. 11 shows the results obtained for different dynamical parameters after the orbit integration on the bootstrapped sample for one single star. In this case, these results correspond to 109 Psc, hosting the exoplanet 109 Psc b. Our estimates for the orbital parameters correspond to the median values of the distributions obtained through resampling, with 1σ confidence intervals. These results are shown for illustrative purposes only, as further processing is required to provide the descriptive statistics of the results and offer insights into the actual motion history of our targets. It is worth noting that the distributions are generally smooth and tightly grouped around a central value (as expected from a Gaussian resampling), with relatively narrow confidence intervals, albeit our double resampling procedure accounting for both individual variations and covariate effects, which proves the robustness of our methodology.

[7] See the *Gaia* DR4 content: https://www.cosmos.esa.int/web/gaia/dr4

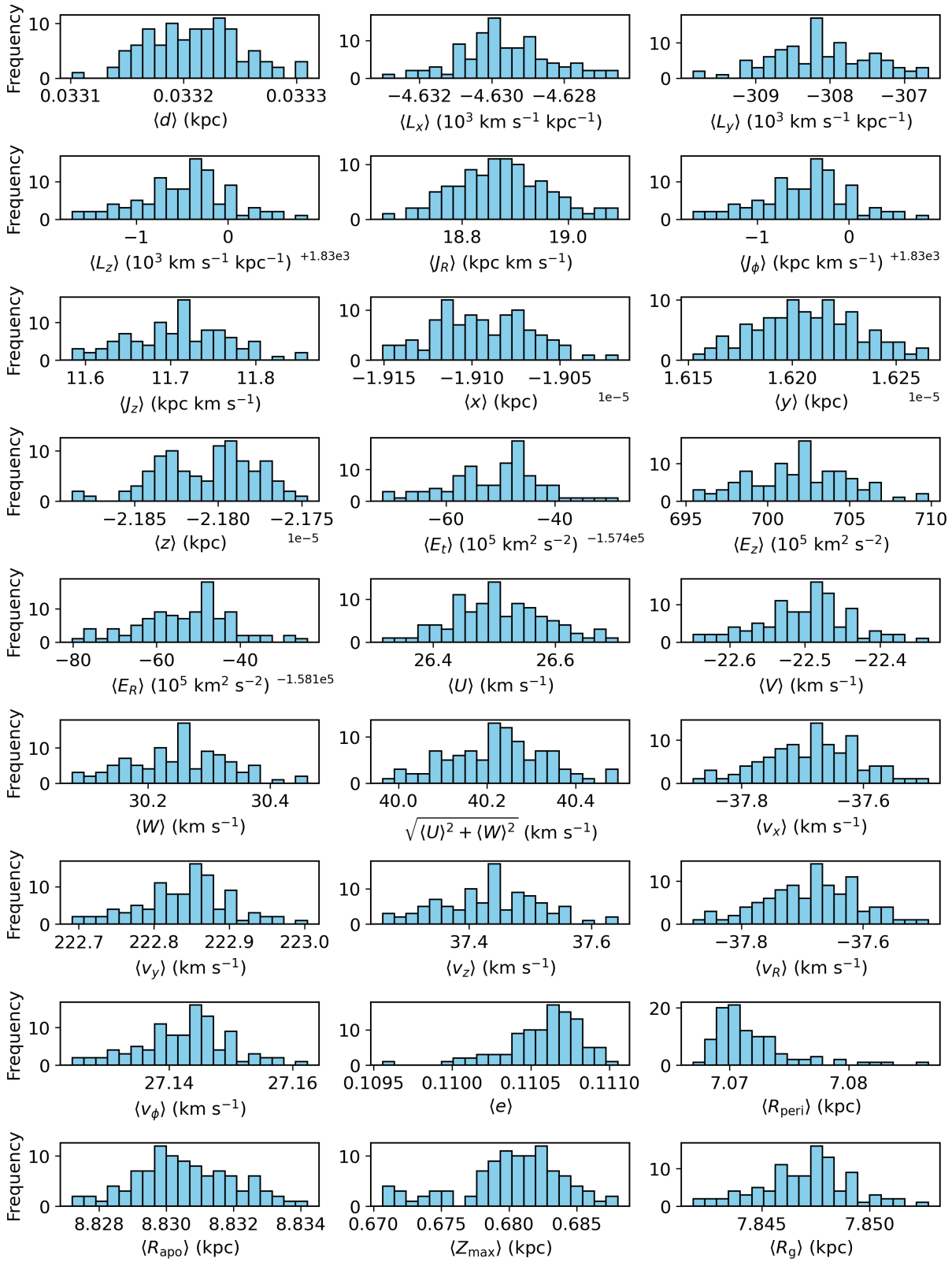

Figure 11: Distributions for several dynamic parameters (see Sect. 2.5) derived from GALPY for 109 Psc. The subplots show the results from our covariance-informed resampling. Distribution widths reflect the full propagation of observational uncertainties, including covariant terms.

4 Conclusions and ongoing work

In this study, we built a consistent catalogue of confirmed exoplanets and their host stars by cross-matching data from the exoplanet.eu catalogue with astrometric and photometric information from *Gaia* DR3, and also 2MASS and AllWise catalogues for intermediate estimations. This dataset enabled the reconstruction of the orbits of a subsample of stars throughout our Galaxy. These results would allow us to understand the influence of stellar migration on planet formation and the characteristics of these systems.

Our main findings and remarks at this stage of the project can be summarised as follows:

1. The need for sufficiently extensive and consistent catalogues has become clearly evident. Current catalogues often combine data from different surveys and contain incomplete parameter sets with missing values. This issue is particularly relevant in the field of exoplanets, where our study is framed. The compilation of exoplanets data covers decades of research, from diverse instruments, observations and techniques, resulting in a highly heterogeneous sample that challenges robust statistical analysis and interpretation.

2. After a brief insight into our final sample of stars hosting exoplanets, we observed stellar parameters reasonably close to solar values, reflecting an expected trend. This is partly due to biases inherent in current exoplanet detection techniques, as well as target selection criteria that often prioritise stars similar to the Sun. These factors influence the nature of the sample and must be considered carefully.

3. Specifically, our sample is comprised of stars with median ages close but slightly younger than the Sun ($\sim$ 4 Gyr), metallicities slightly lower than the Sun, masses peaking at $\sim 1 M_{\odot}$ and temperatures consistent with FGK stars (see the beginning of Sect. 3 for the detailed characterisation of our stellar sample).

With the integration of orbits for our stellar sample now completed, we will process them to combine the results from the bootstrapped orbits and provide final dynamical parameters with confidence intervals and uncertainties. Having the orbits processed, we will be able to characterise the sample dynamically, which will allow us to know whether these stars and their host planets are part of the Galactic disc or the halo (for instance, by building the Toomre and Lindblad diagrams). For those in the Galactic disc, we will be able to compare their current R_g with their R_b and know whether and how much they have migrated (either inward or outward, in case migration is confirmed). In order to do that, we will follow the procedure detailed by Dantas et al. (2025), which entails extrapolating the Galactic chemical enrichment models described by Magrini et al. (2009). To that end, we will make use of a generalised additive model (GAM; introduced by Hastie & Tibshirani, 1990). With the final results for R_g, $R_{\rm apo}$, $R_{\rm peri}$, and the estimated birth radii (R_b), we will be able to compare them, among other dynamical parameters. This will allow us to estimate how much the stars in our sample and their host planets have moved from their R_b. This will provide us insights into the effects of migration (or lack thereof) in the exoplanet population.

Currently, we are assembling a research paper with this study (García-Delgado et al., in prep.) which we intend to submit for publication by the end of 2025. Alongside the paper, we also plan to make the final catalogue publicly available, including all the parameters described along Sec. 2, to enable further studies on this sample. Once the manuscript is submitted to publication, the catalogue will be submitted to the CDS (SIMBAD Astronomical Database) for access by the scientific community[8].

[8]In the meantime, part of the code developed during the project will be available in the GitHub repository: https://github.com/juanjogd/Garcia-Delgado_2025_Do_stars_with_exoplanets_migrate

5 Acknowledgements

I would like to thank my supervisors, Dr. Isabel Rebollido Vázquez and Dr. Maria Luiza Linhares Dantas, for their guidance throughout this project and for their valuable feedback on the manuscript. Their continuous support and availability over the year have been greatly appreciated. I am also grateful to the ESA community at ESAC (Villanueva de la Cañada, Madrid) for their warm welcome and to the PhD students at the Centro de Astrobiología for their helpful advice and encouraging words. I thank the Departamento de Física de la Tierra y Astrofísica at the Universidad Complutense de Madrid for providing access to the HTC service. Special thanks go to Dr. Sergio Pascual Ramírez for his support with the system, for helping with the understanding of its workflow and for assisting with the adaptation of the code to run efficiently on it. I also thank Diego Beltrán for his friendly assistance with some requirements installation involving UNIDAM package and for his accessibility throughout the process.

This work has made use of data from the European Space Agency (ESA) mission *Gaia* (https://www.cosmos.esa.int/gaia), processed by the *Gaia* Data Processing and Analysis Consortium (DPAC, https://www.cosmos.esa.int/web/gaia/dpac/consortium). Funding for the DPAC has been provided by national institutions, in particular the institutions participating in the *Gaia* Multilateral Agreement. This research has made use of data obtained from or tools provided by the portal exoplanet.eu of The Extrasolar Planets Encyclopaedia. This research has made use of the SIMBAD database, operated at CDS, Strasbourg, France. This work made use of the following online platforms: *Slack* (https://slack.com/), *GitHub* (https://github.com/) and *Overleaf* (https://www.overleaf.com/). This work made use of the following PYTHON packages (not previously mentioned): MATPLOTLIB (Hunter, 2007), NUMPY (Harris et al., 2020), PANDAS (McKinney, 2010) and ASTROPY (Astropy Collaboration et al., 2013, 2018, 2022). This work also benefited from TOPCAT (Taylor, 2005).

References

Hastie, T., & Tibshirani, R. (1990). Taylor & Francis. https://books.google.pl/books?id=qa29r1Ze1coC

Wielen, R., Fuchs, B., & Dettbarn, C. (1996). *A&A*, *314*, 438.

Chieffi, A., Limongi, M., & Straniero, O. (1998). *ApJ*, *502*(2), 737–762. https://doi.org/10.1086/305921

Chiappini, C., Matteucci, F., & Romano, D. (2001). *ApJ*, *554*(2), 1044–1058. https://doi.org/10.1086/321427

Santos, N. C., Israelian, G., & Mayor, M. (2001). https://arxiv.org/abs/astro-ph/0109018

Sellwood, J. A., & Binney, J. J. (2002). *MNRAS*, *336*(3), 785–796. https://doi.org/10.1046/j.1365-8711.2002.05806.x

Korn, A. J., Shi, J., & Gehren, T. (2003). *A&A*, *407*, 691–703. https://doi.org/10.1051/0004-6361:20030907

Lépine, J. R. D., Acharova, I. A., & Mishurov, Y. N. (2003). *ApJ*, *589*(1), 210–216. https://doi.org/10.1086/374596

Fischer, D. A., & Valenti, J. (2005). *ApJ*, *622*(2), 1102–1117. https://doi.org/10.1086/428383

Taylor, M. B. (2005, December). In P. Shopbell, M. Britton, & R. Ebert (Eds.), *Astronomical data analysis software and systems xiv* (p. 29, Vol. 347).

Kobayashi, C., Umeda, H., Nomoto, K., Tominaga, N., & Ohkubo, T. (2006). *The Astrophysical Journal*, *653*(2), 1145. https://doi.org/10.1086/508914

Skrutskie, M. F., et al. (2006). *AJ*, *131*(2), 1163–1183. https://doi.org/10.1086/498708
Hunter, J. D. (2007). *Computing in Science & Engineering*, *9*(3), 90–95. https://doi.org/10.1109/MCSE.2007.55
Roškar, R., Debattista, V. P., Quinn, T. R., Stinson, G. S., & Wadsley, J. (2008). *ApJ*, *684*(2), L79. https://doi.org/10.1086/592231
Haywood, M. (2009). *ApJ*, *698*(1), L1–L5. https://doi.org/10.1088/0004-637X/698/1/L1
Magrini, L., Sestito, P., Randich, S., & Galli, D. (2009). *A&A*, *494*(1), 95–108. https://doi.org/10.1051/0004-6361:200810634
Portegies Zwart, S. F. (2009). *The Astrophysical Journal*, *696*(1), L13–L16. https://doi.org/10.1088/0004-637x/696/1/l13
Jordi, C., et al. (2010). *A&A*, *523*, Article A48, A48. https://doi.org/10.1051/0004-6361/201015441
McKinney, W. (2010). In S. van der Walt & J. Millman (Eds.), *Proceedings of the 9th Python in Science Conference* (pp. 56–61). https://doi.org/10.25080/Majora-92bf1922-00a
Schneider, J., et al. (2011). *A&A*, *532*, A79. https://doi.org/10.1051/0004-6361/201116713
Bressan, A., Marigo, P., Girardi, L., Salasnich, B., Dal Cero, C., Rubele, S., & Nanni, A. (2012). *MNRAS*, *427*(1), 127–145. https://doi.org/10.1111/j.1365-2966.2012.21948.x
Gilmore, G., et al. (2012). *The Messenger*, *147*, 25–31.
Roškar, R., Debattista, V. P., Quinn, T. R., & Wadsley, J. (2012). *MNRAS*, *426*(3), 2089–2106. https://doi.org/10.1111/j.1365-2966.2012.21860.x
Astropy Collaboration et al. (2013). *A&A*, *558*, A33. https://doi.org/10.1051/0004-6361/201322068
Minchev, I., Chiappini, C., & Martig, M. (2013). *A&A*, *558*, Article A9, A9. https://doi.org/10.1051/0004-6361/201220189
Randich, S., Gilmore, G., & Gaia-ESO Consortium. (2013). *The Messenger*, *154*, 47–49.
Alexander, R., et al. (2014, January). In H. Beuther, R. S. Klessen, C. P. Dullemond, & T. Henning (Eds.), *Protostars and planets vi* (pp. 475–496). https://doi.org/10.2458/azu_uapress_9780816531240-ch021
Groh, J. H., et al. (2014). *A&A*, *564*, A30. https://doi.org/10.1051/0004-6361/201322573
Bailer-Jones, C. A. L. (2015). *PASP*, *127*(956), 994. https://doi.org/10.1086/683116
Bonanno, A., & Fröhlich, H. .-. (2015). *A&A*, *580*, Article A130, A130. https://doi.org/10.1051/0004-6361/201526419
Bovy, J. (2015). *ApJS*, *216*(2), Article 29, 29. https://doi.org/10.1088/0067-0049/216/2/29
Dayal, P., Cockell, C., Rice, K., & Mazumdar, A. (2015). *ApJ*, *810*(1), Article L2, L2. https://doi.org/10.1088/2041-8205/810/1/L2
Green, G. M., et al. (2015). *The Astrophysical Journal*, *810*(1), 25. https://doi.org/10.1088/0004-637x/810/1/25
Kordopatis, G., et al. (2015). *MNRAS*, *447*(4), 3526–3535. https://doi.org/10.1093/mnras/stu2726
Stonkutė, E., et al. (2016). *MNRAS*, *460*(1), 1131–1146. https://doi.org/10.1093/mnras/stw1011
McMillan, P. J. (2017). *MNRAS*, *465*(1), 76–94. https://doi.org/10.1093/mnras/stw2759
Mints, A., & Hekker, S. (2017). *A&A*, *604*, A108. https://doi.org/10.1051/0004-6361/201630090
Schönrich, R., & McMillan, P. J. (2017). *MNRAS*, *467*(1), 1154–1174. https://doi.org/10.1093/mnras/stx093
Astropy Collaboration et al. (2018). *AJ*, *156*(3), Article 123, 123. https://doi.org/10.3847/1538-3881/aabc4f
Eker, Z., et al. (2018). *MNRAS*, *479*(4), 5491–5511. https://doi.org/10.1093/mnras/sty1834
Frankel, N., Rix, H.-W., Ting, Y.-S., Ness, M., & Hogg, D. W. (2018). *ApJ*, *865*(2), Article 96, 96. https://doi.org/10.3847/1538-4357/aadba5
Green, G. (2018). *The Journal of Open Source Software*, *3*(26), 695. https://doi.org/10.21105/joss.00695
Green, G. M., et al. (2018). *MNRAS*, *478*(1), 651–666. https://doi.org/10.1093/mnras/sty1008

Minchev, I., et al. (2018). *MNRAS*, *481*(2), 1645–1657. https://doi.org/10.1093/mnras/sty2033
Mints, A., & Hekker, S. (2018). *A&A*, *618*, A54. https://doi.org/10.1051/0004-6361/201832739
Ginsburg, A., et al. (2019). *AJ*, *157*, Article 98, 98. https://doi.org/10.3847/1538-3881/aafc33
Haemmerlé, L., et al. (2019). *A&A*, *624*, A137. https://doi.org/10.1051/0004-6361/201935051
Stojković, N., Vukotić, B., Martinović, N., Ćirković, M. M., & Micic, M. (2019). *MNRAS*, *490*(1), 408–416. https://doi.org/10.1093/mnras/stz2519
Feltzing, S., Bowers, J. B., & Agertz, O. (2020). *MNRAS*, *493*(1), 1419–1433. https://doi.org/10.1093/mnras/staa340
Harris, C. R., et al. (2020). *Nature*, *585*(7825), 357–362. https://doi.org/10.1038/s41586-020-2649-2
Tsujimoto, T., & Baba, J. (2020). *ApJ*, *904*(2), Article 137, 137. https://doi.org/10.3847/1538-4357/abc00a
Asplund, M., Amarsi, A. M., & Grevesse, N. (2021). *A&A*, *653*, Article A141, A141. https://doi.org/10.1051/0004-6361/202140445
Cutri, R. M., et al. (2021, February).
Lindegren, L., et al. (2021). *A&A*, *649*, Article A4, A4. https://doi.org/10.1051/0004-6361/202039653
Picogna, G., Ercolano, B., & Espaillat, C. C. (2021). *Monthly Notices of the Royal Astronomical Society*, *508*(3), 3611–3619. https://doi.org/10.1093/mnras/stab2883
Astropy Collaboration et al. (2022). *ApJ*, *935*(2), Article 167, 167. https://doi.org/10.3847/1538-4357/ac7c74
Carr, C., Johnston, K. V., Laporte, C. F. P., & Ness, M. K. (2022). *MNRAS*, *516*(4), 5067–5083. https://doi.org/10.1093/mnras/stac2403
Gilmore, G., et al. (2022). *A&A*, *666*, Article A120, A120. https://doi.org/10.1051/0004-6361/202243134
Randich, S., et al. (2022). *A&A*, *666*, Article A121, A121. https://doi.org/10.1051/0004-6361/202243141
Baba, J., Saitoh, T. R., & Tsujimoto, T. (2023). *Monthly Notices of the Royal Astronomical Society*, *526*(4), 6088–6102. https://doi.org/10.1093/mnras/stad3188
Dantas, M. L. L., et al. (2023). *A&A*, *669*. https://doi.org/10.1051/0004-6361/202243667
Evans, N. R., et al. (2023). *AJ*, *166*(3), Article 109, 109. https://doi.org/10.3847/1538-3881/ace89b
Gaia Collaboration, Vallenari, A., Brown, A. G. A., Prusti, T., et al. (2023). *A&A*, *674*, Article A1, A1. https://doi.org/10.1051/0004-6361/202243940
Komaki, A., Fukuhara, S., Suzuki, T. K., & Yoshida, N. (2023). *arXiv e-prints*, Article arXiv:2304.13316, arXiv:2304.13316. https://doi.org/10.48550/arXiv.2304.13316
Magrini, L., et al. (2023). *A&A*, *669*, Article A119, A119. https://doi.org/10.1051/0004-6361/202244957
Zhang, X., et al. (2023). *MNRAS*, *524*(2), 1855–1884. https://doi.org/10.1093/mnras/stad1941
Baba, J., Tsujimoto, T., & Saitoh, T. R. (2024). *The Astrophysical Journal Letters*, *976*(2), L29. https://doi.org/10.3847/2041-8213/ad9260
Edenhofer, G., et al. (2024). *A&A*, *685*, Article A82, A82. https://doi.org/10.1051/0004-6361/202347628
Lu, Yuxi et al. (2024). *Monthly Notices of the Royal Astronomical Society*, *535*(1), 392–405. https://doi.org/10.1093/mnras/stae2364
Nepal, S., et al. (2024). *A&A*, *681*, Article L8, L8. https://doi.org/10.1051/0004-6361/202348365
Dantas, M. L. L., et al. (2025). *A&A*, *696*, Article A205, A205. https://doi.org/10.1051/0004-6361/202453034
Ofir, A., Yoffe, G., & Aharonson, O. (2025). *The Astronomical Journal*, *169*(2), 90. https://doi.org/10.3847/1538-3881/ad91a7

Portegies Zwart, S., & Huang, S. (2025). *arXiv e-prints*, Article arXiv:2505.13666, arXiv:2505.13666. https://doi.org/10.48550/arXiv.2505.13666